



## Comprehensive two-dimensional gas chromatography for the analysis of Fischer–Tropsch oil products

Rina van der Westhuizen<sup>a,b</sup>, Renier Crous<sup>a</sup>, André de Villiers<sup>b</sup>, Pat Sandra<sup>b,\*</sup>

<sup>a</sup> Sasol Technology R&D, PO Box 1183, Sasolburg 1183, South Africa

<sup>b</sup> Stellenbosch University, Private Bag X1, Matieland 7602, South Africa

### ARTICLE INFO

#### Article history:

Received 31 August 2010

Accepted 25 October 2010

Available online 30 October 2010

#### Keywords:

One-dimensional GC

Comprehensive two-dimensional GC

Fischer–Tropsch oils

Anderson–Schultz–Flory selectivity model

Trace analysis

### ABSTRACT

The Fischer–Tropsch (FT) process involves a series of catalysed reactions of carbon monoxide and hydrogen, originating from coal, natural gas or biomass, leading to a variety of synthetic chemicals and fuels. The benefits of comprehensive two-dimensional gas chromatography (GC × GC) compared to one-dimensional GC (1D-GC) for the detailed investigation of the oil products of low and high temperature FT processes are presented. GC × GC provides more accurate quantitative data to construct Anderson–Schultz–Flory (ASF) selectivity models that correlate the FT product distribution with reaction variables. On the other hand, the high peak capacity and sensitivity of GC × GC allow the detailed study of components present at trace level. Analyses of the aromatic and oxygenated fractions of a high temperature FT (HT-FT) process are presented. GC × GC data have been used to optimise or tune the HT-FT process by using a lab-scale micro-FT-reactor.

© 2010 Elsevier B.V. All rights reserved.

### 1. Introduction

The Fischer–Tropsch (FT) process is a polymerisation reaction that produces a vast number of compounds over a wide carbon number range. During product work-up, more than 200 industrial chemicals are produced in addition to various grades of fuels (petrol, diesel, jet fuel, etc.) [1]. The fuels are practically free of sulphur- and nitrogen-containing compounds, which make them environmental friendly compared to crude oil derivatives.

FT products are distributed over a number of phases. For high temperature processes (HT-FT, with reactor temperatures between 300 °C and 380 °C), products are spread over gas, oil and water phases with only small amounts of wax formed. For low temperature processes (LT-FT, reactor temperatures between 200 °C and 250 °C), the average chain length of the product is higher and more waxes are produced. The analysis of any one of these phases is very challenging. This study addresses the analysis of the complex oil products.

The FT-oil product spectrum is dependent on reaction variables like the reactor system used, temperature, pressure, catalyst formulation, etc. LT-FT processes result in a relatively un-complicated product spectrum with comparatively high average carbon numbers (up to around C<sub>120</sub>) and mostly linear primary FT products. For HT-FT a much more complex product is obtained. At elevated reac-

tion temperatures the reaction rate increases and the average chain length of the molecules is reduced with a corresponding increase in methane formation. Secondary product formation (a result of primary FT products that re-adsorb on the catalyst surface and undergo further reaction) is enhanced, resulting in much higher complexity due to the presence of thousands of secondary reaction products at trace levels.

Fundamental studies are aimed at understanding the reactions that take place at the catalyst surface with the ultimate goal of optimising FT processes. Predictive models were developed to estimate consumption of reactants and the distribution of products with variables such as temperature, partial pressures, catalyst promoter content, etc. Kinetic models are used to predict the consumption of reactants, whereas selectivity modelling is used to describe the product distribution [2].

Complete predictive models for FT product distributions are not available. The Anderson–Schulz–Flory (ASF) model is a mathematical model for homogeneous polymerisation that has been formulated by Schulz [3] and Flory [4] and extended for chain branching by Friedel and Anderson [5]. This model is often used to characterise FT products and several studies have shown that the FT product spectrum approximately follows this model, although with some deviations [6–8]. According to this model, product distributions can be described by a single parameter namely the chain growth probability  $\alpha$ :

$$\frac{S_n}{n} = \alpha^n \frac{(1 - \alpha)^2}{\alpha} \quad (1)$$

\* Corresponding author.

E-mail address: [pat.sandra@richrom.com](mailto:pat.sandra@richrom.com) (P. Sandra).

$$\ln\left(\frac{S_n}{n}\right) = n \ln \alpha + \ln \frac{(1-\alpha)^2}{\alpha} \quad (2)$$

where  $S_n$  is the mass (weight) fraction of products with carbon number  $n$ . The chain growth probability factor  $\alpha$  reflects the probability that a molecule will continue reacting to form a longer chain.  $\alpha$  is largely determined by the catalyst and the specific process conditions. A logarithmic plot of the mass fraction per carbon number versus the carbon number will give a straight line. The  $\alpha$ -values are determined from the slopes of the plots and can vary between 0 and 1. In an ideal polymerisation reaction  $\alpha$  will be constant and independent of the carbon number.

The majority of ASF plots for Fischer–Tropsch products show a nearly straight line in the region from  $C_4$  and  $C_{12}$ . A break in the ASF trend line in the region around  $C_{12}$ – $C_{13}$  has been observed with either higher or lower  $\alpha$ -values for longer chain products. In addition, deviations from linearity have also been noted in the  $C_1$ – $C_3$  range i.e. methane levels are normally higher and  $C_2$  compounds lower than predicted. Various studies aiming to explain these deviations are often contradictory [6–15].

Until now, one-dimensional GC (1D-GC) was exclusively used in studies of FT selectivity models and their deviations [2,13,14,7,6,16–18]. A number of authors have questioned the accuracy of the GC results used, although no systematic investigation of this aspect has been reported. 1D-GC, even using the most recent high-efficiency capillary columns, provides peak capacities in the order of ~500–600 [19]. For highly complex samples such as HT-FT products, with components present at low ppm (mg/kg) levels, the data used for these studies (and the accuracy of the models themselves) are therefore questionable. Comprehensive two-dimensional GC (GC  $\times$  GC) provides a number of advantages compared to 1D-GC. Peak capacities for GC  $\times$  GC are in the order of tens of thousands (the product of the peak capacities of two columns of different selectivity). Moreover, peaks are often arranged in highly ordered and structured plots, where peaks belonging to homologous series are positioned along straight lines on the retention plane. GC  $\times$  GC is therefore extensively used to characterise petroleum fractions [20–23]. High peak capacity and ordered plots should result in much better quantification compared to 1D-GC to construct ASF selectivity models. To the best of our knowledge, a comparison of 1D-GC and GC  $\times$  GC in this respect has not yet been reported.

An additional benefit of GC  $\times$  GC is an increase in sensitivity (up to 10-fold) compared to 1D-GC. This is a result of the very fast separation achieved in the second dimension column that minimizes peak broadening and effectively increases the signal-to-noise ratio [22,24]. The sensitivity issue is of less of importance for LT-FT product characterization as the oils consist of only a few hundred, mainly linear primary FT components at percentage levels. On the other hand, sensitivity is of utmost importance for the analysis of HT-FT oils where the highly complex product spectrum contains thousands of primary and secondary components. Moreover, several components or compound classes are only present at trace levels but their presence and quantities are extremely important to optimise and fine-tune the FT process and to study their formation (primary or secondary FT product). In a previous contribution, we described the characterization of dienes in an HT-FT derived product by GC  $\times$  GC–TOF-MS. Dienes are prone to polymerisation by Diels–Alder reactions and dimers and trimers were detected in the 2-D plot by operating the MS in the ion extraction mode [25]. Polymerisation is thought to be partially responsible for gum formation in HT-FT-derived products. The analyses of aromatic precursors and aromatic sub-classes and of oxygenates in HT-FT products by GC  $\times$  GC are presented. Both classes could not be studied in the past because of a high degree of peak overlap in 1D-GC. Lab-scale micro-FT-reactor experiments are described to illustrate the use of

GC  $\times$  GC to monitor the formation of both classes in function of the temperature.

## 2. Experimental

### 2.1. Samples and reactor experiments

The LT- and HT-FT samples were experimental samples from Sasol Technology R&D, Sasolburg, South Africa. Lab-scale micro-FT-reactor experiments were performed at constant pressure and feed gas ratios. Experiments were performed at reaction temperatures of 320 °C, 350 °C and 380 °C. Samples of the oils were taken off-line from heated knock-out pots.

### 2.2. Analytical conditions

1D-GC analyses were performed on a 7890A Gas Chromatograph equipped with a 5975 inert mass selective detector (MS) and a flame ionisation detector (FID) from Agilent Technologies (Little Falls, DE, USA). The MS was used for identification purposes and the FID for quantification. A 30 m  $\times$  250  $\mu$ m ID  $\times$  1  $\mu$ m d<sub>f</sub> HP-1 (Agilent Technologies) was used with a temperature program of 40 °C (0.2 min), ramped at 2 °C/min to 350 °C. A constant helium gas flow of 1.2 mL/min was maintained with a split ratio of 100:1. The injection volume was 0.1  $\mu$ L.

GC  $\times$  GC was performed using a Pegasus 4D instrument equipped with a time-of-flight mass spectrometer (TOF-MS) and an FID detector (Leco Corporation, St. Joseph, MI, USA). The first dimension column was a 30 m  $\times$  250  $\mu$ m  $\times$  0.25  $\mu$ m RTX-Wax (Restek) with a temperature program of 40 °C (0.2 min), ramped at 3 °C/min to 245 °C. The second dimension column was a 1.8 m  $\times$  100  $\mu$ m  $\times$  0.1  $\mu$ m RTX-5 (Restek), and the second oven followed the first oven with a lead of 25 °C. The modulation period was 7 s. The carrier gas was helium at a constant flow of 1.2 mL/min. Injection volume was 0.1  $\mu$ L with a split ratio of 400:1. TOF-MS was used for identification of compounds or selective ion extraction while the FID was used for quantification. TOF-MS and FID data were collected at 100 spectra (points)/s. To enable direct comparison of GC  $\times$  GC and 1D-GC results, quantification was performed by normalization of peak areas. Relevant response factors were used for oxygenated compounds while a response factor of unity was assumed for hydrocarbons. Quantification using GC  $\times$  GC–FID data was performed using ChromaTOF software (Leco, v4.21).

## 3. Results and discussion

### 3.1. 1D-GC and GC $\times$ GC analysis of Fischer–Tropsch oils

Petrochemical products are amongst the most complex products. Blomberg et al. [20] estimated the number of compounds in a crude oil-derived middle distillate to be more than  $10^6$ . FT product streams are less complex than crude-derived products but can still contain tens of thousands of compounds. Note that O-containing compounds are present in FT oils but not S- and N-containing compounds.

LT-FT oils are relatively simple and composed of mainly primary linear molecules present at percentage levels and very little secondary reaction products. However, a high degree of component co-elution is already observed in 1D-GC analysis. The co-elution is not necessarily the result of the limited peak capacity of the column but rather of a shared physical property. For instance, if the volatility of two compounds is very close and the polarity different, they may co-elute on a column in which separation is based on volatility only, even though the total number of peaks in the sample may be much lower than the peak capacity of the column. Moreover,

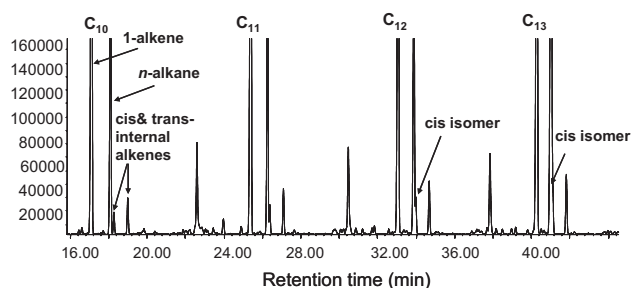


Fig. 1. Part of the 1D-GC chromatogram for a LT-FT oil.

selectivity of a column for specific classes decreases in function of the temperature and/or temperature program rate. An example is shown for the analysis of a LT-FT oil on the non-polar (boiling point separation) HP-1 column under common GC conditions (Fig. 1).

For the  $C_{10}$ -group, the 1-alkene elutes before the  $n$ -alkane followed by the cis-internal alkene and the trans-internal alkene. The cis-2-internal alkene peaks elute closer to the  $n$ -alkane peaks with increasing carbon number and from  $C_{12}$  onwards they are completely obscured. This results in an overestimation of the alkanes and an underestimation of the internal alkenes. Branched isomers of paraffins, olefins and oxygenates also elute in the same area of the GC chromatogram. To distinguish between these classes, it is necessary to identify each of the peaks in the chromatogram and sum them. Especially ketones, aldehydes and acids are not easily identified because these low-level peaks also elute in the same region as branched isomers.

Co-elution of peaks occurs to an even larger extent when 1D-GC is performed on a polar column (e.g. RTX-Wax). Alkanes and alkenes elute early from these columns because of their non-polar nature and as a result their resolution is worse than obtained on a non-polar column. While the internal alkenes are separated from the  $n$ -alkanes on this column, they co-elute with the branched isomers and oxygenates. This results in overestimation of internal alkenes and underestimation of branched isomers and oxygenates. Thus even for a product containing relatively few compounds, quantitative results may differ significantly between two columns of different selectivities.

In contrast, by combining the two selectivities in the reversed GC  $\times$  GC mode, complete separation of the different compound classes is obtained and even branched and linear isomers are separated (Fig. 2). Separation in the two-dimensional separation plane occurs according to both boiling point and polarity differences, resulting in a group-type separation of the different classes of compounds.

GC  $\times$  GC profiling of fuels is commonly performed on what is called the normal phase GC  $\times$  GC mode i.e. a non-polar column in

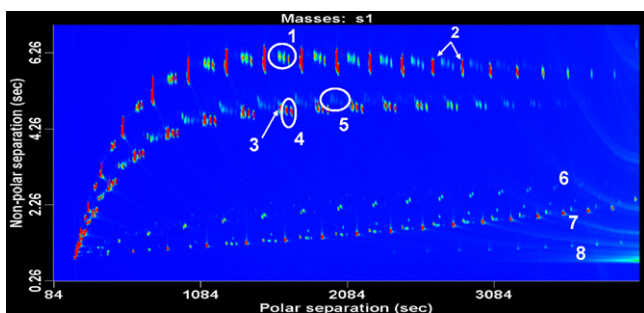


Fig. 2. GC  $\times$  GC-FID analysis of a LT-FT oil. Numbering: (1) branched alkanes, (2)  $n$ -alkanes, (3) 1-alkenes, (4) 2-alkenes, (5) branched alkenes, (6) linear and branched ketones and aldehydes, (7) linear and branched alcohols and (8) linear and branched acids.

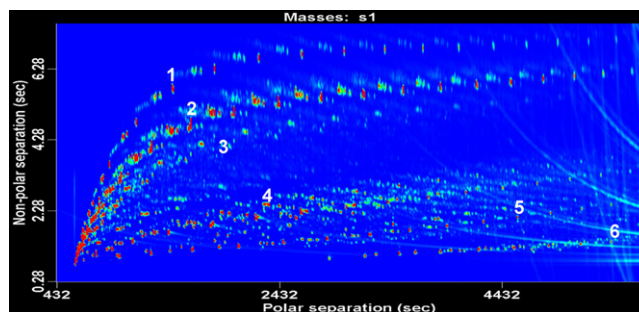


Fig. 3. GC  $\times$  GC-FID analysis of a HT-FT oil. Numbering: (1)  $C_{12}$  alkanes, (2)  $C_{12}$  alkenes, (3)  $C_{12}$  cyclic aliphatics, (4)  $C_{12}$  aromatics, (5)  $C_{12}$  alcohols and (6)  $C_{12}$  acids.

the first dimension and a polar column in the second dimension. The reversed GC  $\times$  GC mode i.e. a polar column (BPX50) in the first dimension and a non-polar column in the second dimension was used by Vendeuvre et al. [26] for better characterization of the aromatic fraction of petroleum middle-distillates. For FT-products the highest orthogonality and by far the best class separation of alkenes, aromatics and oxygenates is obtained with a WAX column as first column [26] as obvious from Fig. 2. Peak identification and accurate quantification are drastically improved by using GC  $\times$  GC compared to 1D-GC because peak co-elution is significantly reduced even for relatively simple mixtures as LT-FT oils.

For HT-FT oils, more than 650 compounds can be detected by 1D-GC analysis on a 60 m non-polar capillary column but this is completely insufficient to unravel its complexity. By using a polar column in the first dimension and a 1.8 m non-polar column in the second dimension, the peak capacity is ca. 15,000 ( $600 \times 25$ ) and the complete 2D separation space is utilised. The different classes of alkanes, alkenes, cyclics, aromatics, alcohols and acids are ordered as illustrated for  $C_{12}$  in Fig. 3.

### 3.2. Comparison of quantitative results of 1D-GC and GC $\times$ GC for HT-FT oil.

In 1D-GC co-eluting peaks of different carbon numbers are grouped together giving incorrect carbon number distributions. As an example, on a non-polar column separation in the region between the  $C_7$  and  $C_8$   $n$ -alkanes, one would also find  $C_8$  branched alkane and alkene compounds,  $C_7$  and  $C_8$  cyclic aliphatics,  $C_5$  alcohols,  $C_6$  ketones and aldehydes,  $C_4$  acids and  $C_7$  aromatic molecules. These peaks would be quantified together as  $C_8$  branched compounds. As a result, the total amount for a specific carbon number is either overestimated or underestimated. In contrast, in GC  $\times$  GC the individual chemical classes and their branched and cyclic isomers are all separated in two dimensions and accurate carbon numbers can be assigned. A comparison of the carbon number distributions for 1-alkenes and for the total product distribution obtained by 1D-GC and GC  $\times$  GC of a HT-FT oil shows a huge overestimation of  $C_5$ – $C_7$  compounds and an underestimation for higher boiling compounds by 1-D GC (Fig. 4).

These quantitative differences have a strong influence on the ASF plots. Fig. 5 compares the ASF plots for the 1-alkene and total product carbon distributions for 1-D GC and GC  $\times$  GC data. The deviation from linearity in the  $C_1$ – $C_6$  region is because only the oil phase of the HT-FT product was analyzed and the contribution of the gaseous fraction was excluded. A nearly straight line is observed from  $C_7$  to  $C_{20}$  for the 1-alkenes for both methods, but with a slight offset between the two graphs. A larger deviation is noted in the lower carbon number region as a result of the overestimation of 1-alkenes by 1-D GC. This deviation is much clearer for the carbon distribution of the total product, where the plot shows a significant downward trend in the region  $C_7$ – $C_{20}$  for the 1-D GC

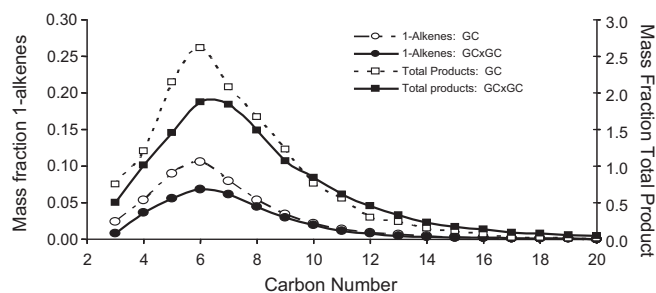


**Fig. 4.** Comparison of the carbon distributions of the total HT-FT product and 1-alkenes obtained by 1D-GC and GC  $\times$  GC.

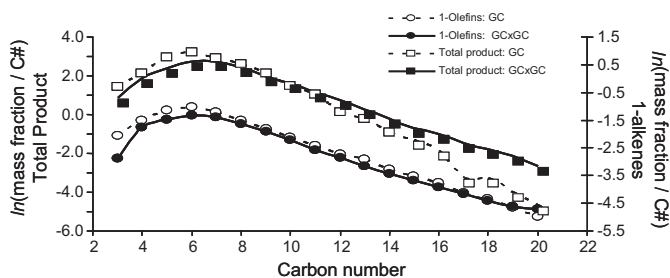


**Fig. 5.** Comparison of ASF plots of the total HT-FT product and 1-alkenes obtained by 1D-GC and GC  $\times$  GC.

data. Accordingly, the slopes of these graphs, which represent  $\alpha$ -values, also differ. The  $\alpha$ -value from the GC  $\times$  GC analysis is 0.7458. The equation for the straight part of the line (from  $C_7$  to  $C_{20}$ ) was  $y = -0.2933x + 2.7030$  with a  $R^2$ -value of 0.9985. The 1D GC-data gave an  $\alpha$ -value of 0.6577 with  $y = -0.419x + 3.8942$  and  $R^2 = 0.9923$ .

It can be concluded that the  $\alpha$ -values traditionally used for HT-FT selectivity models and based on 1D-GC results are inaccurate. Deviations from linearity of ASF plots previously reported by various authors [6–8], can therefore at least in part be attributed to analytical error caused by the high degree of peak co-elution in the 1-D GC methods exclusively used in the past to construct ASF plots.

### 3.3. Application of GC $\times$ GC to follow primary and secondary product formation in HT-FT products

Primary and secondary FT product formation is of utmost importance to optimise FT processes and has been studied by a number of authors [2,7]. By using shorter residence times (removing products from the reactor before secondary reactions can take place) and low space velocities (the relation between volumetric flow and reactor volume), secondary reactions can be suppressed and primary FT products elucidated. In this manner, linear 1-alkenes and  $n$ -alkanes were identified as primary FT products, while the formation of branched hydrocarbons is believed to proceed via both primary and secondary routes. Linear alcohols and aldehydes are generally regarded as primary FT products, whereas the formation of acids and ketones are thought to be either primary or secondary reactions [2]. Olefin co-feeding studies have indicated that olefins can act as chain initiators and that double bond shifts of 1-alkenes can occur [27–32]. Olefins can re-adsorb on the catalyst surface and undergo secondary reactions such as hydrogenation, hydroformylation, hydrogenolysis, etc. Like the alkenes, alcohols can re-adsorb on the catalyst surface and undergo secondary reactions. Alkanes and alkenes are dehydrogenated to form aromatics in secondary reactions at the severe conditions of the HT-FT process [2]. Very little information is available in the literature regarding the nature and formation of aromatics and oxygenates.

The general trend in FT processes is that with increasing reaction temperature, an increase in degree of branching, cyclization and formation of aromatics, is observed with a corresponding decrease in total aliphatic content. At HT-FT reaction conditions, more than half the product spectrum can be of a secondary nature. GC  $\times$  GC in combination with a lab-scale micro reactor is particularly useful to monitor the evolution of secondary products as a function of reaction conditions, since this cannot be done accurately using conventional 1-D GC methods.

Valuable new information was obtained from GC  $\times$  GC data regarding aromatics in HT-FT products. The aromatic pre-cursor groups of cyclic alkenes, dienes and cyclic dienes, as well as aromatic sub-classes of mononuclear and binuclear aromatics are separated by GC  $\times$  GC. Higher polyaromatic hydrocarbons are only present at trace level in FT products. The procedure to analyze aromatic precursors and the correspondingly formed aromatic compound is illustrated for  $C_7$  (Fig. 6A). An ion extracted chro-

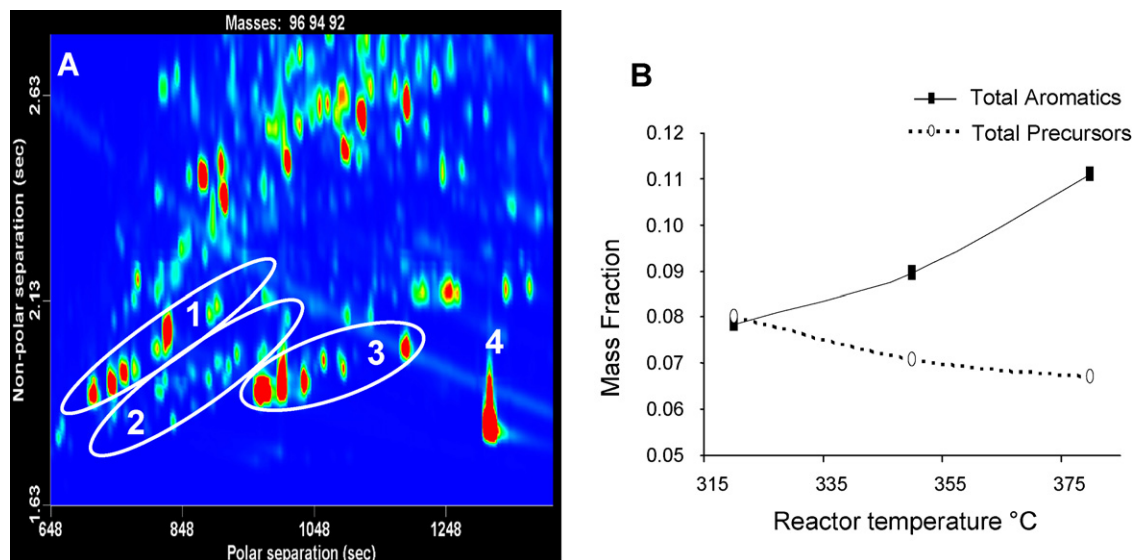


**Fig. 6.** (A) Extracted ion contour plot for the  $C_7$  aromatic precursors (1–3) and toluene (4). (B) Evolution of total aromatics and aromatic precursors as a function of reaction temperature.

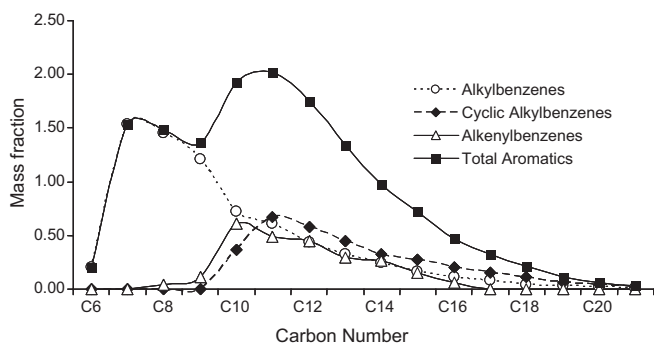


Fig. 7. The mononuclear aromatic distribution of an HT-FT oil.

matogram is constructed using  $m/z$  96 for the  $C_7$ -cyclic alkenes and  $C_7$ -dienes (note that both classes are separated in reversed mode GC  $\times$  GC),  $m/z$  94 for the  $C_7$ -cyclic dienes and  $m/z$  92 for the formed aromatic compound, in this case toluene. The mass fractions in function of temperature are presented in Fig. 6B. As expected, the precursors decrease and the aromatics increase in function of temperature.

The same procedure was used to elucidate all aromatic substances in HT-FT oil and on constructing the distribution curve for total mononuclear aromatics, an interesting observation was made that would not have been possible without the help of GC  $\times$  GC. As opposed to the normal distribution usually found for all other component classes in FT products, two maxima were noted in the distribution curve. Fig. 7 shows the curves for the total aromatic mass fraction together with the curves for the most abundant classes i.e. the alkylbenzenes, the cyclic alkylbenzenes and the alkenylbenzenes. Further investigation showed that aromatic subclasses each display unique carbon number distributions, and that these are responsible for the two maxima observed in the total aromatic distribution. The first maximum is due to the alkylbenzenes and the second mainly to the cyclic alkylbenzenes and alkenylbenzenes. Such detailed information on aromatics is particularly valuable for fuels where the aromatic structure influences fuel properties like density, cetane number, cold flow properties, etc.

In 1D-GC, low level oxygenate peaks are hidden underneath the complex hydrocarbon primary level peaks resulting in an underestimation of their mass fraction. Reversed mode GC  $\times$  GC is ideally suited to separate low level oxygenated species and to study the correlation of their formation with increasing reaction tempera-

ture. Fig. 8A shows the complexity of a relevant part of the HT-FT contour plot for the alcohols, aldehydes and ketones with elucidation of the primary, branched, cyclic and secondary alcohols. For most oxygenates, like with the aliphatic hydrocarbons, there is an increase in secondary product formation and a corresponding decrease in primary FT products with increasing temperature. Fig. 8B shows the effect of reaction temperature in the range of 320–380 °C on the alcohol fraction. The primary FT 1-alcohols and cyclic alcohols decrease in concentration while the branched and secondary alcohols increase with temperature. The observed decrease in cyclic alcohols is due to their conversion to phenols and other aromatic alcohols.

Similar trends were observed for other oxygenates. As expected, primary aldehydes decrease with increasing temperature while ketones, which are secondary reaction products, increase in concentration with increasing temperature. An increase in the formation of branched and cyclic carbonyls was also observed. Note that although the primary oxygenated products decrease with increasing temperature, the total amount of oxygenates increases.

The trends for acid formation are more difficult to understand. There is an increase in the formation of branched acids with increasing temperature, but cyclic acids were not observed. Other experimental factors such as the types and levels of alkali promoter as well as ageing of the catalyst are known to affect acid formation [2].

#### 4. Conclusions

GC  $\times$  GC in the reversed mode provides valuable information about FT products that has not previously been available. The complete two-dimensional separation plane is utilised and the different compound classes and sub-classes are separated based on both volatility and polarity differences. Quantitative data from GC  $\times$  GC analysis showed that deviations from linearity in ASF plots in the region from  $C_7$  to  $C_{20}$  are based on co-elution when 1D-GC is applied.

The formation of secondary reaction compounds like aromatics could be studied by evaluating the trends in the formation of aromatic precursors and sub-classes with increasing reaction temperatures. Two maxima in the total aromatic distribution have been detected for the first time as a result of sub-group distributions that are formed within the mononuclear aromatic class. This would have been impossible to detect without the high peak capacity of GC  $\times$  GC. Moreover, by the high sensitivity of GC  $\times$  GC compounds present at trace level like the oxygenates could be

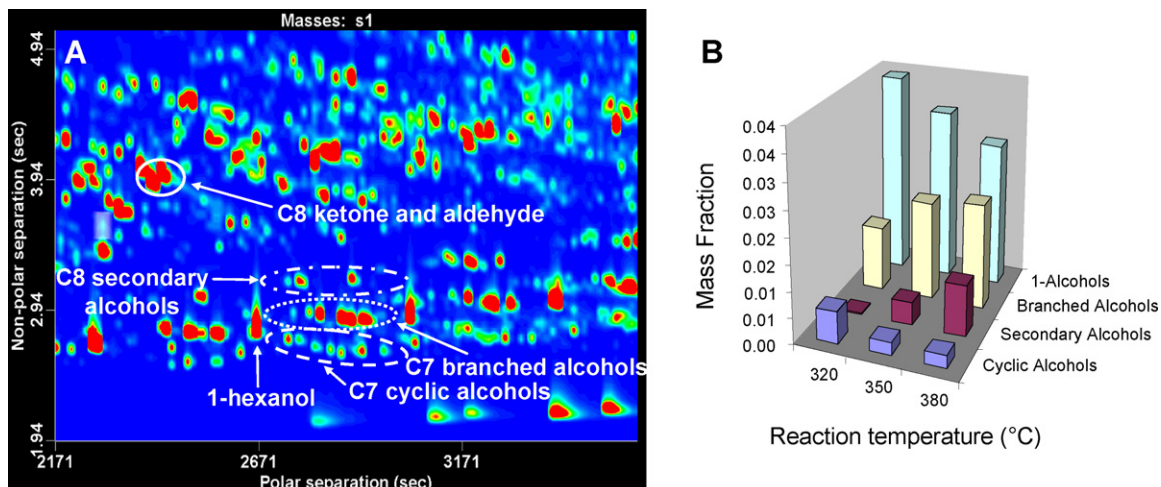


Fig. 8. (A) Part of the FID contour plot with the aldehydes, ketones and alcohols. (B) Changes in levels of alcohols in function of temperature.

studied. The information deduced from GC × GC analyses allows the optimisation of plant conditions to produce more high-value fuels and chemicals.

## References

- [1] J. Collings, *Mind over Matter – The Sasol Story. A Half-century of Technology Innovation*, Johannesburg, South Africa, 2002, p4.
- [2] A. Steynberg, M.E. Dry, *Stud. Surf. Sci. Catal.* 152 (2004) 406.
- [3] G.V. Schulz, *Z. Phys. Chem.* B30 (1935) 379.
- [4] P. Flory, *J. Am. Chem. Soc.* 58 (1936) 1877.
- [5] R.A. Friedel, R.B. Anderson, *J. Am. Chem. Soc.* 72 (1950) 2307.
- [6] I. Puskas, R.S. Hurlburt, *Catal. Today* 84 (2003) 99.
- [7] H. Schulz, M. Claeys, *Appl. Catal.* 186 (1999) 71.
- [8] J. Patzlaff, Y. Liu, C. Graffmann, J. Graube, *Catal. Today* 71 (2002) 381.
- [9] R. Snel, *Catal. Lett.* 1 (1988) 327.
- [10] Y. Yang, S. Pen, B. Zhong, Q. Wang, *Catal. Lett.* 19 (1993) 351.
- [11] G.P. van der Laan, A.C.M. Beenackers, *Ind. Eng. Chem. Res.* 38 (1999) 1277.
- [12] X. Zhan, B.H. Davis, *Petrol. Sci. Technol.* 18 (2000) 1037.
- [13] Y. Ji, H. Xiang, J. Yang, Y. Xu, Y. Li, B. Zhong, *Appl. Catal. A* 214 (2001) 77.
- [14] G.P. Van der Laan, *Kinetics, Selectivity and Scale Up of the Fischer–Tropsch Synthesis*, Ph.D. Thesis, Rijksuniversiteit Groningen, 1999.
- [15] B. Shi, B. Davis, *Appl. Catal. A* 277 (2004) 61.
- [16] E.W. Kuipers, C. Scheper, J.H. Wilson, I.H. Vinkenburg, H. Oosterbeek, *J. Catal.* 158 (1996) 288.
- [17] G.A. Huff, C.N. Satterfield, *J. Catal.* 85 (1984) 370.
- [18] H.G. Strenger, *J. Catal.* 92 (1985) 426.
- [19] L.M. Blumberg, W.H. Wilson, M.S. Klee, *J. Chromatogr. A* 894 (1999) 15.
- [20] J. Blumberg, P.J. Schoenmakers, J. Beens, R. Tijssen, *J. High Resol. Chromatogr.* 20 (1997) 539.
- [21] J. Beens, H. Boelens, R. Tijssen, J. Blumberg, *J. High Resol. Chromatogr.* 21 (1998) 47.
- [22] J. Dalluge, J. Beens, U.A.Th. Brinkman, *J. Chromatogr. A* 1000 (2003) 69.
- [23] M. Adahchour, J. Beens, R.J.J. Vreuls, U.A.Th. Brinkman, *TrAC* 25 (2006) 726.
- [24] P.J. Marriott, R. Shellie, *TrAC* 21 (2002) 573.
- [25] R. Van der Westhuizen, A. Crouch, P. Sandra, *J. Sep. Sci.* 31 (2008) 3423.
- [26] C. Vendeuvre, R. Ruiz-Guerrero, F. Bertoncini, L. Duval, D. Thiebaut, M.-C. Hennion, *J. Chromatogr. A* 1086 (2005) 21.
- [27] O. Johnston, R. Joyner, *Stud. Surf. Sci. Catal.* 75 (1993) 165.
- [28] E. Iglesia, S.C. Reyes, R.J. Madon, S.L. Soled, *Adv. Catal.* 39 (2) (1993) 221.
- [29] H. Schulz, M. Claeys, *Appl. Catal. A: Gen.* 186 (1999) 71.
- [30] J.H. Boelee, J.M.G. Custers, K. van der Wiele, *Appl. Catal.* 53 (1999) 1.
- [31] K. Fujimoto, *Top. Catal.* 2 (1995) 259.
- [32] H. Schulz, Zh. Nie, *Stud. Surf. Sci. Catal.* 136 (2001) 159.